Effect of the dissolved pressurizing gas on the pressure surge during the filling process of spacecraft feedlines

Bombardieri Cristiano, Traudt Tobias, Manfletti Chiara
DLR Lampoldshausen, Department of Rocket Propulsion, Germany

ABSTRACT

During the start-up of the propulsion system of a satellite or spacecraft, the opening of the tank isolation valve will cause the propellant to flow into an evacuated feedline and slam against a closed valve, inducing severe pressure peaks.
An experimental campaign is performed at DLR Lampoldshausen to better investigate this filling process. Tests run with saturated and deareated fluids clearly show the influence of the pressurizing gas on the water hammer pressure profile. To gain further insight of this aspect, a quartz pipe is installed at the dead-end and high speed imaging has been performed.

1 INTRODUCTION

During the start-up of the propulsion system of a satellite or spacecraft, the opening of the tank isolation valve will cause the propellant to flow into an evacuated feedline and slam against a closed thruster valve. This filling process, called priming, can cause severe pressure peaks that could lead to structural failure. In the case of monopropellants such as hydrazine also the risk of adiabatic compression detonation must be taken into account in the design of the feedline subsystem.
To prevent these two potential hazards, the solution is to slow down the flow through the use of either a flow restriction device (venturi [1] [2] or orifice [3] [4]) or the gas cushion effect. However, the addition of flow restriction devices increases the system pressure loss. For some missions, a small amount of gaseous helium is loaded into the feedline subsystem downstream of the closed latch valves. It acts as a cushion to the liquid front and proves to be an effective way to decrease the surge pressure [1].
The phenomenon of priming involves complex two-phase flow: the liquid entering the evacuated pipe undergoes flash evaporation creating a vapor cushion in front of the liquid that mixes with the residual inert gas, usually helium. Moreover, the dissolved pressurizing gas in the liquid will desorb making the priming process difficult to model numerically. For these reasons, priming and/or water hammer tests are always part of the qualification campaign of the propulsion subsystem of a satellite or spacecraft that uses storable propellants.
Gibec and Maisonneuve [5] performed water hammer experiments with real propellants, namely MMH, NTO and hydrazine, for different pipe geometries including straight, bend, elbow and tee pipes. They hypothesized that phenomena such as cavitation, pipe deformation and vapor pressure may interfere with the water hammer.
Lecourt and Steelant [6] performed several test with ethanol, acetaldehyde and MMH for straight and bend pipes. They observed a surprising multiple steps evolution of the first pressure peak and provided a possible explanation. They also demonstrated that ethanol can be used as a replacement fluid instead of toxic MMH.

Lema et al. [7] investigated the effect of a fully saturated liquid compared to a deareated one in vacuum conditions. Test results showed that for the saturated liquid the pressure peak is slightly smaller due to the desorption of the dissolved gas which acts as a cushion in front of the liquid. Flow visualization with high speed imaging was also conducted by means of a quartz pipe at the dead-end.

These last two references ([6] [7]) are in particular the basis for the present work. More in details, the target of this work is to evaluate the effect of the dissolved pressurizing gas on the water hammer pressure profile by comparing it with the deareated case. The effect is found to be closely related to the step-plateau shape observed in [6]. To gain further insight of this aspect, a quartz pipe has been installed at the dead-end and high speed imaging up to 19,200 fps has been performed. The image analysis proves to give an extreme valuable information to better understanding this complex transient phenomenon and thanks to them a possible explanation of the first pressure peak profile is given.

2 EXPERIMENTAL APPARATUS

2.1 Test Bench description

In order to investigate and gain detailed insight into the phenomena of priming a new test bench has been built at DLR Lampoldshausen. The test bench features a 80 liters run tank pressurized up to 50 bar, a flexible pressurization system (GN2 or GHe as a pressurizing gas) as well as a modular test section with its own conditioning system. This modularity ensures that the test bench is not limited to one test section but it can reproduce the real operating feedline system geometry. Conditioning of the test section can be either done via evacuation or pressurization. The test bench is equipped with a fast opening valve (FOV), pneumatically actuated.

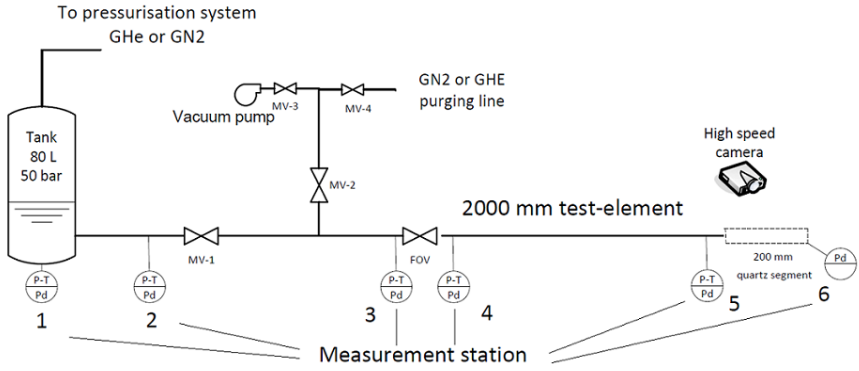

Figure 1 : Schematic of *M3.5 Fluid Transient Test-Bench* at DLR Lampoldshausen

Schematic of the test facility is shown in Figure 1. The geometry of the test-element is a 2000 mm straight stainless steel pipe with a relative large outer diameter (3/4 inch or 19.05 mm) in order to examine high mass flow that are typical of spacecraft feedlines like the ESA automatic transfer vehicle ATV. The wall thickness of the test section is 1.25 mm (ID 16.56mm). At five points it is mounted onto a rigid support structure to limit its movements. The support structure is made of aluminum profiles. The test section

is mounted with a downward slope of about 1° to facilitate the purging procedure. The upstream part, from the tank to the valve, is a 22x1.5 mm straight stainless steel pipe. For the conditioning of the test-element, a tee piece is inserted 550 mm downstream the tank, which is further diverted into two lines to allow purging and evacuation procedure. Detailed geometry of the test-bench is given in Table 1.

Table 1: Dimensions of the test-bench

Description	
Test section length (incl. quartz segment)	*2200 mm*
Quartz segment length	*200 mm*
Upstream pipe tank-FOV	*1023 mm*
Position of T-branch from tank	*550 mm*
Test section inner pipe diameter	*16.56 mm*
Test section outer pipe diameter	*19.05mm*

2.1.1 Fast opening valve

As reported in previous works ([6] [7] [8]), the valve opening should be faster than the impact time of the liquid front at the dead-end. In other words, the valve must be fully open before the liquid reaches the end of the test-element pipe. The impact time, as shown later, is in the range 140-150 ms. As a fast opening valve, a co-axial valve is chosen. It is pneumatic actuated (up to 40 bar actuation pressure) and its opening time is only 6 ms. The valve seat is 16mm and its pressure loss coefficient is 12.5. The valve is mounted on a rigid support to limit vibrations during the opening.

The valve opening transient is of importance for numerical validation. It is an important boundary condition although its value not always available. A requirement for the experimental set-up was therefore to have a position measurement sensor not only to ensure reproducibility of the valve opening transient but also to provide the necessary input for numerical simulations. The valve features a position encoder, and its opening profile (an example in Figure 2) has been perfectly reproducible over all the performed tests.

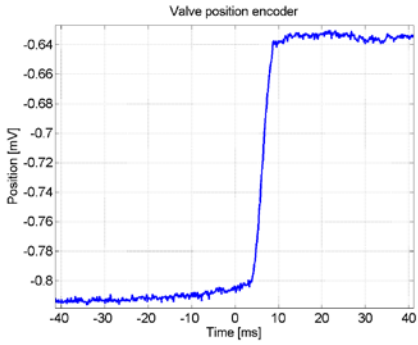

Figure 2: Position signal of the valve opening transient. Complete opening is achieved in only 6 ms

2.1.2 Sensors

Measurements of pressure and temperature are performed at 6 different stations as shown in Figure 1. Each measurement station consists of 3 transducers: one thermocouple type K, 1 KHz sampling rate; one absolute piezoresistive pressure sensor type 4043A200 from Kistler, 10 KHz sampling rate; one dynamic piezoelectric pressure sensor type 601A from Kistler, 150 KHz sampling rate.
To avoid aliasing and high-frequency noise, the filter of the dynamic pressure sensors has been set to 30 KHz.
Sensors are screw in a 20 mm thick disk with the same inner diameter of the pipe to avoid flow disturbances. Dynamic pressure sensors (5.5 mm diameter) and thermocouple are flush mounted, while the absolute pressure sensor is 2 mm beneath the surface through a 1mm bore. The measurement stations are located as follows:

• pos. 1 : at the tank

• pos. 2 : 250 mm downstream of the tank

• pos. 3 : 318 mm upstream of the FOV

• pos. 4 : 160 mm downstream of the FOV

• pos. 5 : 1990 mm downstream of the FOV

• pos.6 : at the end (only dynamic pressure)

In the tests without the quartz segment, stations 5 and 6 are replaced by one single measurement module with a screw adapter to the pipe (weld-on Swagelok type) as depicted in Figure 3. The inner diameter of the adapter has been re-worked so that a constant inner diameter without step (that might cause turbulence and induce flow perturbation) is obtained.

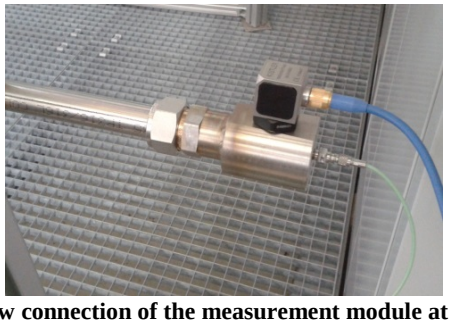

Figure 3 Screw connection of the measurement module at the dead-end

2.1.3 High speed camera

A Photron Fastcam SA-X is used for image acquisition. The following settings are used for the video images presented in this paper:

- Frame rate: 19,200 fps
- Shutter: 1/30769 s
- Resolution: 1024x184

The optical segment is a quartz pipe, 200 mm long and with an inner and outer diameter of 16.56 mm and 31 mm respectively. It is installed at the end of the test section as showed in Figure 4.

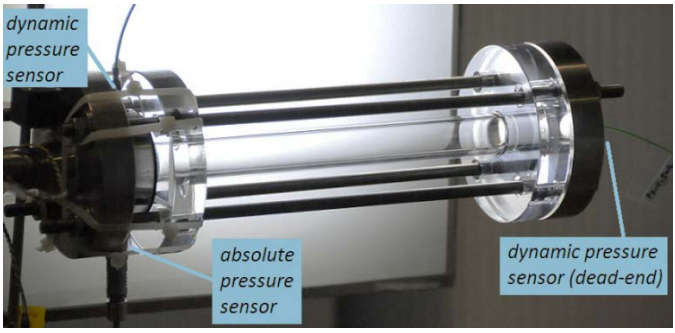

Figure 4: Quartz segment used for high speed imaging installed at the dead-end

2.2 Test procedure

Before each test the downstream line is purged with a gaseous nitrogen (GN2) flow by opening MV-4 and MV-2 (see Figure 1) and unscrewing the measurement module at the test-element end. After this operation, the test-section is evacuated by means of a vacuum pump (MV-3 open) to the desired vacuum level. The fast opening valve (FOV) and MV-2 are then closed and MV-1 is opened to manually prime the upstream pipe. At this point, automatic operations are performed by the controlling software: the tank pressure is set at a given value (with GHe or GN2), FOV opens (time: 0 ms) and at the same time the trigger command for data acquisition and the camera is given. Data are recorded for 4 seconds.

For the deareated case, the vacuum pump is connected to the tank gas supply line and the pressure is lowered to almost the saturation value of the liquid. The pump is then disconnected and the tank pressure slowly build-up due to the dissolved gas being released. The pump is again switched on and this procedure is repeated until the tank pressure is stable near the saturation pressure.

2.3 Test matrix

First, tests with different pressures in the test-element, labelled as P_{line} , are performed, while the tank pressure is kept at 20 bar. The P_{line} for water and ethanol has been set so that the same ratio with respect to their saturation pressure is kept. The vacuum pressure levels are shown in Table 2, named Test Campaign A. The residual gas in the line is nitrogen (GN2).

Then, Test Campaign B is carried out to investigate the effect of the pressurizing gas. Deareated and saturated liquid are compared both at vacuum condition in the line.

Table 2: Test matrix: line pressure for water and ethanol tests (Test Campaign A, top); pressurizing gas tank conditions (Test Campaign B, bottom)

Test Campaign A
P tank : 20 bar

Water (P_{sat} 19.2 mbar) P_{line}	**Ethanol (P_{sat} 40.6 mbar) P_{line}**
300 mbar (P_{sat} x15)	430 mbar (P_{sat} x11)
100 mbar (P_{sat} x5)	200 mbar (P_{sat} x5)
50 mbar (P_{sat} x2.5)	100 mbar (P_{sat} x2.5)
10 mbar (P_{sat} x0.5)	20 mbar (P_{sat} x0.5)

Test Campaign B
P tank : 20 bar

Water P_{line} 10 mbar	**Ethanol P_{line} 20 mbar**
Deareated	Deareated
Saturated GN2 20bar	Saturated GN2 (20 bar)
Saturated GHE 20bar	
Forced GN2 injection	

Tests are repeated three times for each test conditions to examine reproducibility. Figure 5 shows an example of the reproducibility achieved. The measured pressure peak difference among the three tests is less than 1.5%. From an experimental point of view, reproducibility at vacuum condition with deareated liquid is somewhat better than the saturated case.

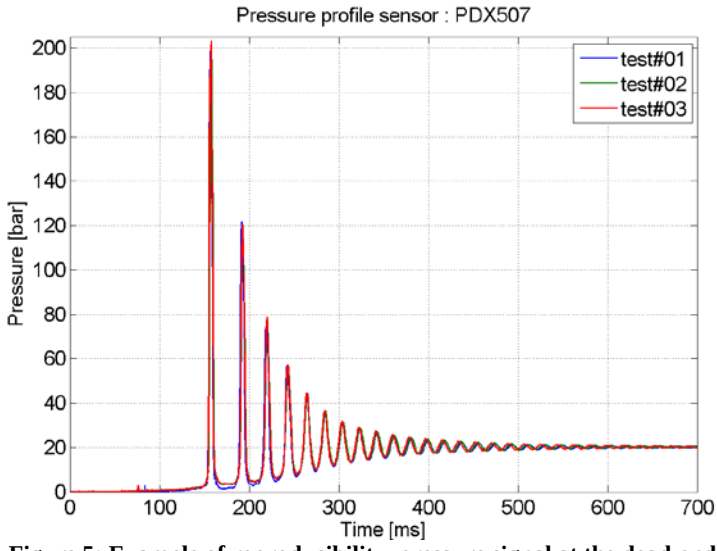

Figure 5: Example of reproducibility, pressure signal at the dead-end

3 TEST RESULTS

The target of the experimental campaign is to reproduce the filling process occurring in a spacecraft feedline system. The results of the tests will provide a database to be used for the validation of numerical simulations. From an engineering point of view, three parameters are of importance to the designer: pressure peak, frequency of the oscillation and damping characteristics. All these parameters depend on fluid properties such as density and speed of sound.
However, the density and the speed of sound are not constant in the fluid. Calculation of the speed of sound is a difficult task, because of the two-phase flow nature of the process. Trapped gas volumes or entrained free gas bubbles greatly complicate the calculation of the acoustic wave speed [9]. In addition, when injected in the evacuated line, the saturated propellant will desorb the pressurizing gas at a given rate, the amount of the latter being usually not known and not easily estimated. All that makes the acoustic wave speed a function of both pressure and time.
The purpose of the present paper is instead to analyse qualitatively the pressure peak and to evaluate the effects of the dissolved pressurizing gas on it.
For all the tests, the fast acting valve opens at 0 ms, the water hammer phenomenon takes place and it damps out in 500-700 ms, depending on the operating conditions.

3.1 Effect of line pressure

The effect of the line initial pressure is depicted in Figure 6 for water and ethanol. As expected, the pressure peak increases with decreasing line pressure, and so does the frequency of the oscillations. The time at which the pressure peak occurs is also sooner.
After the first peak, no column separation takes place as the amount of residual gas in the line is too high and thus preventing the pressure from dropping to the saturation value.
When the line pressure level approaches the saturation pressure of the liquid ($P_{line} = P_{sat}$ x 2.5), the difference between the pressure peak is small (red curve and cyan curve): 194 vs 198 bar respectively for water; 121 and 129 for ethanol. At this conditions in fact, the liquid undergoes flash boiling and the amount of the generated vapour outcomes the residual inert gas.
Further tests performed with water at line pressure lower than 20 mbar (20-15-10-5 mbar) proved in fact that no difference in the pressure peak is visible.
In the case of water, the first pressure peak becomes rougher with a peculiar profile that will be discussed in the next section.

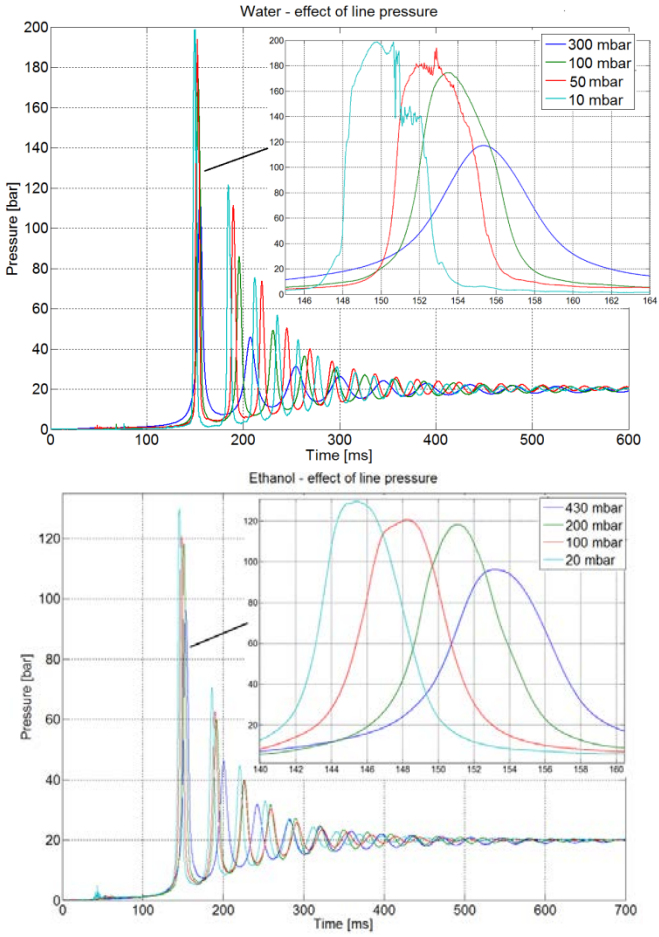

Figure 6 : Effect of the line pressure. Water (top) is pressurized with GN2, while ethanol (bottom) is pressurized with GHe

3.2 Test with deareated and saturated liquid

When the fluid is primed into the evacuated line, it will not only undergo flash boiling, but it will also release the dissolved pressurizing gas (desorption) at a given rate. In a similar way, when the pressure rises some of the released gas will be absorpted back into the fluid. However the absorption is rather a slow process compared to the desorption.

In his work, Lema et al. [7] experimentally showed that for a saturated liquid the pressure peak is lower than the deareated case. Due to the gas desorption, the pressure peak also occurs slightly later and the wave damps out faster thanks to the larger volume of gas.

In order to evaluate the effect of the pressurizing gas, tests are performed with deareated fluid vs saturated one. As explained in Section 2.2, in the case of deareated fluid, the tank is vacuum pumped until saturation pressure is achieved and stable. Then it is fast

pressurized with GHe and tests are run few seconds later, so that no GHe is dissolved in the liquid.
Figure 7 shows the first pressure peak for the two conditions. When the fluid is deareated the pressure profile is smoother than the saturated condition for both the liquids.

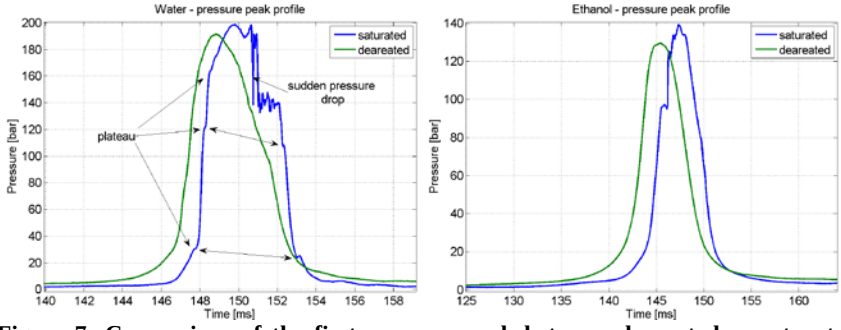

Figure 7: Comparison of the first pressure peak between deareated vs saturated liquid for water (left) and ethanol (right)

The saturated pressure peak also occurs 2 ms later. This is explained by the released dissolved gas that acts as a cushion slowing down the liquid front. The same effect would also indicate a lower pressure peak. Experimentally however the pressure peak for the saturated case is slightly higher than the deareated one, being respectively 198 vs 192 bar for water and 139 vs 129 bar for ethanol. The reason for this is unclear, although an hypothesis can be formulated. As it will be described later in Section 3.4 with the support of high speed imaging, in the case of saturated liquid, the gas desorption will cause gas pockets in the fluid forming multiple liquid slugs. These slugs would move ahead of the main flow and therefore the tank pressure would act on a smaller amount of liquid mass resulting in a slightly higher acceleration, thus a slightly higher impact velocity. It should be noted that also the valve pressure losses play an important role on the cavitation phenomenon. Tests with the quartz pipe installed just downstream the valve are being performed at present to qualitatively confirm this hypothesis.

In the saturated case, an interesting pressure profile with multiple steps is observed. Each is followed by a very fast plateau of <0.1 ms and similarly, also the down-slope presents a symmetrical profile with two plateaux almost at the same pressure level as the up-slope. This peculiar shape has also been noticed in previous experiments performed by Lecourt and Steelant [6]. The authors postulated that this multiple step increase is related to two-phase flow phenomena, such as cavitation, condensation and mixing of the liquid with the residual non-condensable gas in the line.
At around 151 ms a sudden pressure drop from 200 to 140 bar takes place. This could be due to the gas bubble collapsing that creates an additional volume for the liquid causing an expansion and therefore a pressure drop. This negative pressure gradient seems too severe to be caused by fluid-structure interaction. The reason for it remains unclear, and it has been observed that it only happens with saturated fluid.

In the case of water, additional tests with water saturated with GHe have also been run. The pressure profile has less pronounced steps and it is somehow in between the GN2 saturated and deareated conditions (Figure 8). This could have been expected as the solubility of GHe in water is much lower than the GN2 one.

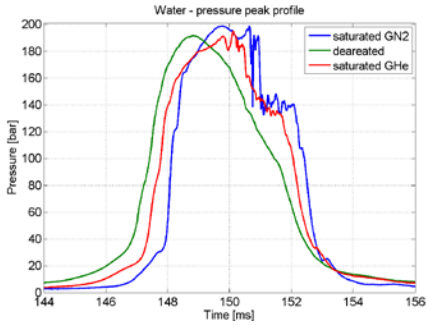

Figure 8: Comparison among deareated water and saturated case with GHe vs GN2

3.3 Test with forced injected GN2

3.3.1 Procedure

To better investigate the effect of the dissolved gas, a different pressurizing technique is performed in the case of water. Instead of the usual pressurization from the top of the vessel, the GN2 is now injected from the bottom of the vessel so that it flows through the liquid and mix with it. GN2 is blown for one hour into the tank at 23 bar while the tank is kept at 20 bar by means of a pressure regulator valve. In this way not only the liquid will be saturated, but also free gas bubbles will be entrained in water. Tests are then run after different waiting times to evaluate the effect of the decreasing amount of non-dissolved GN2. With respect to the legend in Figure 9, the waiting times of the tests are as follows:

1. test#1: just immediately after the GN2 injection
2. test#2: after 1h
3. test#3: after 3 h
4. test#4: after 24 h

The initial line pressure is 10 mbar for all the tests.
The tank is kept at 20 bar over all the tests, so it can be assumed that the amount of dissolved GN2 in the liquid is constant and equal to the maximum value at this pressure. The amount of non-dissolved gas is instead decreasing with time. Free gas bubbles can be retained on the tank wall and in small surface imperfections (welding points, junctions, sensor surfaces). Part of them will move towards the ullage volume of the tank due to non-equilibrium conditions and pressure perturbations during the tests. In this respect, the forced injection of GN2 can be seen as a way to add extra GN2 beyond the maximum absorption quantity.

3.3.2 Description of the pressure evolution

Results of the tests are shown in Figure 9. To facilitate the description of the pressure evolution, A represents the first peak and B the second peak.
Test#1 has a first peak A1 of quite a low pressure value (100 bar), while the second peak B1 is occurring rather sooner than it should (with respect to the standard case, at about 185 ms) and with a steep rise. That may indicate that A1 and B1 are not separated pressure peaks, but instead are both part of the same pressure rise.
Test#2 shows in fact that peaks A1 and B1 moved closer, resulting in peak A2 and B2, where now B2 is higher than B1. In the next test#3 the two peaks have merged together, so that A2 becomes A3 and it is now a plateau, while the peak B3 increases again in magnitude. Finally, after 24h, the pressure shape (test#4) tends to the standard case, where the plateau A3 becomes A4, now of shorter duration (<.3 ms) and the pressure peak reaches 200 bar as the standard saturated case.

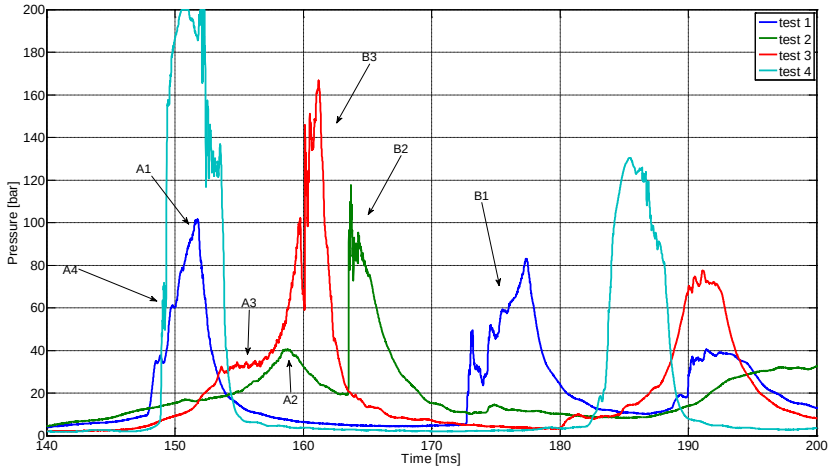

Figure 9: Pressure evolution at different waiting time upon injection of GN2 from the bottom of the tank

From the above description of the pressure evolution, the pressure step profile is found as a two-phase flow effect due not to the residual gas in the line as hypothesized in [6], but to the dissolved pressurizing gas into the liquid. Lecourt and Steelant [6] described the pressure evolution of the first peak as (possibly) due to different physical processes, assuming the adiabatic compression of the residual gas and the vapour bubble finite time to collapse to be responsible for the multiple steps. However, the adiabatic compression of the residual gas does not seem to play a role in causing the step profile being the amount of residual gas the same both in the deareated case and in the saturated case. In addition, they speculated about the influence of the absorption/desorption of the pressurizing gas, a fact that is experimentally confirmed in this present work.
In order to understand the mechanism that causes the step profile, a model is proposed in the next paragraph thanks to the support of high speed imaging.

3.4 High speed imaging analysis

To gain further insight of the priming process, a 200 mm quartz pipe with the same inner diameter of the test-section is placed at the dead-end and high speed imaging is performed at 19,200 fps. For safety reason, the tank pressure is reduced at 8 bar and different line pressures are set. The vacuum case with saturated water is showed in Figure 10 and hereafter commented. The pressure signal depicted in Figure 10 refers to the dead-end sensor.
At around 100 ms after the valve opening, some pressure spikes occur: these are due to single droplets (image 1) that precede the main flow and hit the sensor surface. The flow is stratified due to the gravity, the liquid wets the bottom of the pipe (2) and after slamming at the end turns back filling the top. At this stage the pressure is still low (1.3 bar) and not rising yet. The flow gradually increases until it the whole diameter is wet (3) and the quartz segment is now completely filled with liquid-gas mixture (4). The pressure reaches a first local maximum (5) of 18 bar, drops to 15 bar (6) and then a second slug of liquid compress the existing liquid-gas mixture (7). The arrival of this liquid slug is clearly visible at the left side of the quartz segment, where the liquid comes in: the dense gas cloud moves rapidly towards right (6-7). The pressure reaches then the maximum value of 45 bar (8). This frame (8) is in fact the brightest indicating that the liquid

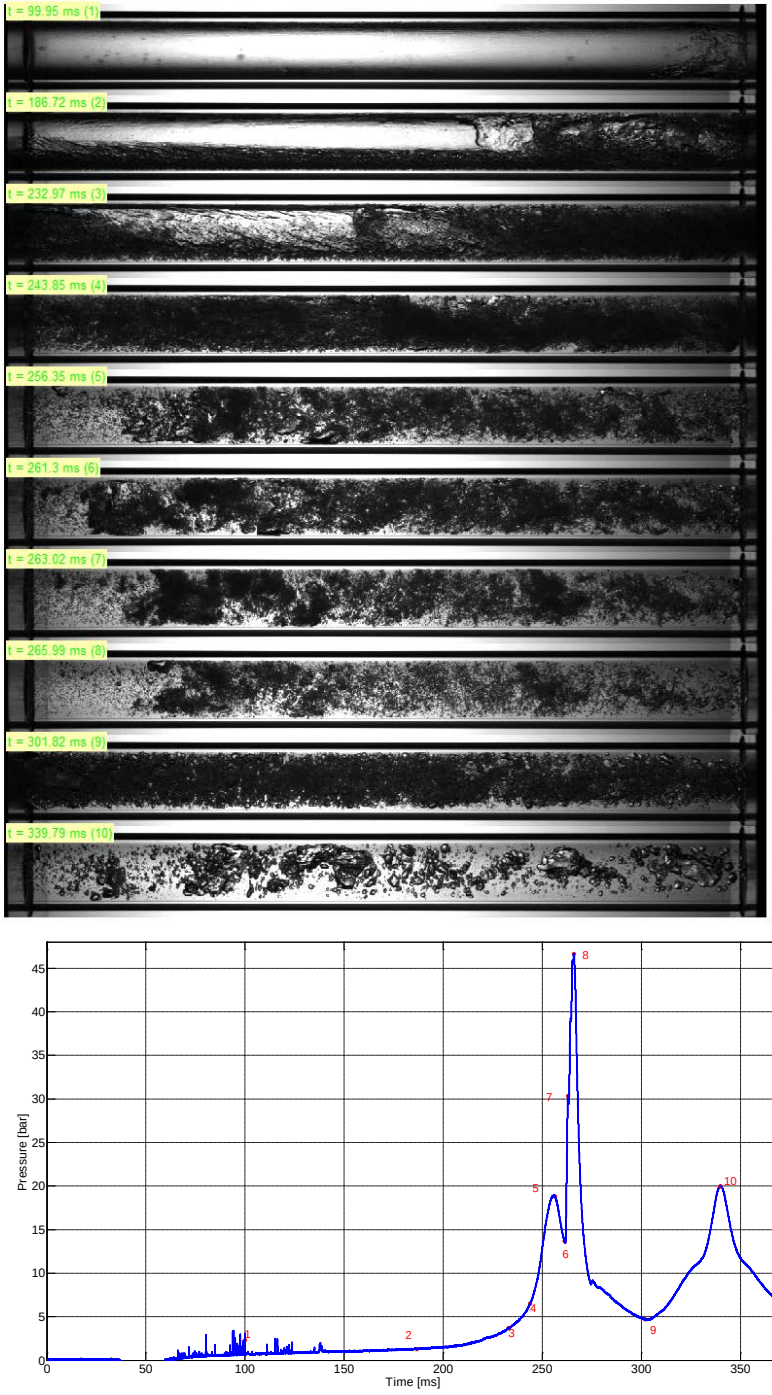

Figure 10: Video frames and pressure signal for saturated water, P_{line}: 10 mbar

amount by volume is the highest and the gas bubbles are tiny, still in a cloud form. As the wave moves upstream towards the tank, the pressure drops to 6 bar (9). Now the flow is fully bubbly. The pressure wave is then travelling from the tank and the pressure increases again (10). At the second pressure peak the bubbles have a bigger size and will move slowly upwards to the top of the pipe due to the gravity.
From the imaging analysis, the crucial point is the arrival of a second liquid slug (6-7) that provided an explanation for the pressure peak profile.
The authors hypothesize that the same mechanism occurs at the high pressure case, causing the aforementioned step-plateau profile. At 20 bar, since the driving pressure is higher, the small and fast pressure drop (5-6) will evolve in the plateau previously described. The idea is that the desorption of the dissolved gas will create gas pocket inside the liquid, and the later could be modelled as multiple separated slugs that impinge one on the others resulting in the step-plateau profile.

Numerical simulations may help to verify this hypothesis. In this respect, preliminary numerical work [10] has underlined the necessity of sub-models that take the absorption/desorption dynamics into account, the importance of which has been experimentally confirmed in the present paper. Moreover, the use of 1D model might be inadequate to describe the transient as the imaging analysis clearly showed that the flow is stratified (image 2-3).

4 CONCLUSIONS

At DLR Lampoldshausen a new test facility to investigate fluid transient phenomena has been built and in detail described. Purpose of this new test facility is to reproduce the filling processes occurring in spacecraft and satellite feedlines during the start-up transient. Several priming test in both pre-pressurized and evacuated pipeline have been performed with water and ethanol, being the latter the best replacement fluid for the toxic hydrazine.
First, the effect of the line pressure is investigated. Decreasing the line pressure causes a higher water hammer pressure peak at the dead-end. However, when the line pressure drops near and below the saturation pressure of the liquid, no more change in the pressure profile have been measured for both liquids. In this case in fact the flash boiling of the liquid produce a vapour amount that is predominant compared to the residual gas in the line and thus a further decrease of the line pressure does not affect the pressure peak.
Experiments with saturated and deareated liquid have also been performed. In the case of saturated liquid, an interesting pressure evolution with multiple step-plateaux has been observed for both fluids. When the liquid is deareated the pressure profile is au contraire smooth. In order to understand the causes of this pressure evolution, a flow of GN2 is injected from the bottom of the tank so that a not negligible amount of non-dissolved gas in form of free bubbles is entrained in the liquid. Tests are then run after different waiting time to compare the effect of the decreasing amount of non-dissolved gas. Results allow to detect a clear evolution of the pressure profile with the waiting time, and providing so an explanation for the plateau characteristic.
Furthermore, high speed imaging by means of a quartz segment is performed in case of saturated water. With the support of the image analysis a possible interpretation of the pressure profile has been provided.
Future experiments will focus on the effect of different geometries like tees, bend and elbow in order to reproduce the real geometry of a spacecraft feedline system.

5 BIBLIOGRAPHY

[1] H. C. Hearn, “Development and application of a priming surge analysis methodology,” in *41st AIAA/ASME/SAE/ASEE Joint Propulsion Conference & Exhibit*, 2005.

[2] A. Scroggins, “A Streamlined Approach to Venturi Sizing,” in *48th AIAA/ASME/SAE/ASEE Joint Propulsion Conference & Exhibit*, Atlanta, Georgia, 2012.

[3] C. Y. Joh and K. D. Park, “Pressure surge analysis and reduction in the KOMPSAT propellant feed system,” in *Proceedings KORUS 2000. The 4th Korea-Russia International Symposium on Science and Technology*, 2000.

[4] M. J. Morgan, “Pressure transient characterization test for Star-2 propulsion system fuel manifold,” in *40th AIAA/ASME/SAE/ASEE Joint Propulsion Conference & Exhibit*, Fort Lauderdale, Florida, 2004.

[5] I. Gibek and Y. Maisonneuve, “Water Hammer Tests with Real Propellants,” *AIAA*, vol. 4081, 2005.

[6] R. Lecourt and J. Steelant, “Experimental Investigation of Waterhammer in Simplified Basic Pipes of Satellite Propulsion Systems,” *AIAA*, no. 2007-5532, July 2007.

[7] M.Lema and J.Steelant, “Experimental Characterization of the Priming Phase using a Propellant Line mock-up,” *Space Propulsion Conference, Bordeaux, France*, May, 8 2012.

[8] T. Lin and D. Baker, “Analysis and Testing of Propellant Feed System Priming Process,” *Journal of Propulsion and Power*, vol. 11, pp. 505-512, 1995.

[9] V. Streeter and E. Wylie, Fluid Transient, Michigan, USA: FEB Press, 1983.

[10] C. Bombardieri, T. Traudt and C. Manfletti, “Experimental and Numerical Analysis of Water Hammer during the Filling Process of Pipelines,” *Space Propulsion Conference, Cologne, Germany*, May 2014.